

Dependence of mechanical properties on the site occupancy of ternary alloying elements in γ'-Ni_3Al: *Ab initio* description for shear and tensile deformation

Minru Wen(文敏儒), Xing Xie(谢兴), Huafeng Dong(董华锋), Fugen Wu(吴福根), Chong-Yu Wang(王崇愚)

Citation: Chin. Phys. B . 2020, 29(7): 078103 . **doi:** 10.1088/1674-1056/ab8a38
Journal homepage: http://cpb.iphy.ac.cn; http://iopscience.iop.org/cpb

What follows is a list of articles you may be interested in

Prediction of structured void-containing 1T-$PtTe_2$ monolayer with potential catalytic activity for hydrogen evolution reaction

Bao Lei(雷宝), Yu-Yang Zhang(张余洋), Shi-Xuan Du(杜世萱)

Chin. Phys. B . 2020, 29(5): 058104 . **doi:** 10.1088/1674-1056/ab8203

Controllable precision of the projective truncation approximation for Green's functions

Peng Fan(范鹏), Ning-Hua Tong(同宁华)

Chin. Phys. B . 2019, 28(4): 047102 . **doi:** 10.1088/1674-1056/28/4/047102

Site preferences of alloying transition metal elements in Ni-based superalloy: A first-principles study

Baokun Lu(路宝坤), Chong-Yu Wang(王崇愚), Zhihui Du(都志辉)

Chin. Phys. B . 2018, 27(9): 097102 . **doi:** 10.1088/1674-1056/27/9/097102

The effects of combining alloying elements on the elastic properties of γ-Ni in Ni-based superalloy: High-throughput first-principles calculations

Baokun Lu(路宝坤), Chongyu Wang(王崇愚)

Chin. Phys. B . 2018, 27(7): 077104 . **doi:** 10.1088/1674-1056/27/7/077104

Electronic and mechanical properties of half-metallic half-Heusler compounds CoCr*Z* (*Z*=S, Se, and Te)

Hai-Ming Huang(黄海铭), Chuan-Kun Zhang(张传坤), Ze-Dong He(贺泽东), Jun Zhang(张俊), Jun-Tao Yang(杨俊涛), Shi-Jun Luo(罗时军)

Chin. Phys. B . 2018, 27(1): 017103 . **doi:** 10.1088/1674-1056/27/1/017103

Dependence of mechanical properties on the site occupancy of ternary alloying elements in γ'-Ni_3Al: *Ab initio* description for shear and tensile deformation*

Minru Wen(文敏儒)[1], Xing Xie(谢兴)[1], Huafeng Dong(董华锋)[1,†], Fugen Wu(吴福根)[2], and Chong-Yu Wang(王崇愚)[3,‡]

[1] *School of Physics and Optoelectronic Engineering, Guangdong University of Technology, Guangzhou* 510006, *China*
[2] *School of Materials and Energy, Guangdong University of Technology, Guangzhou* 510006, *China*
[3] *Department of Physics, Tsinghua University, Beijing* 100084, *China*

(Received 12 February 2020; revised manuscript received 8 April 2020; accepted manuscript online 17 April 2020)

The site occupancy behavior of ternary alloying elements in γ'-Ni_3Al (a key strengthening phase of commercial Ni-based single-crystal superalloys) can change with temperature and alloy composition owing to the effect of entropy. Using a total-energy method based on density functional theory, the dependence of tensile and shear behaviors on the site preference of alloying elements in γ'-Ni_3Al were investigated in detail. Our results demonstrate that Fe, Ru, and Ir can significantly improve the ideal tensile and shear strength of the γ' phase when occupying the Al site, with Ru resulting in the strongest enhancement. In contrast, elements with fully filled d orbitals (*i.e.*, Cu, Zn, Ag, and Cd) are expected to reduce the ideal tensile and shear strength. The calculated stress–strain relationships of Ni_3Al alloys indicate that none of the alloying elements can simultaneously increase the ideal strength of the γ' phase for both Ni1-site and Ni2-site substitutions. In addition, the charge redistribution and the bond length of the alloying elements and host atoms during the tensile and shear processes are analyzed to unveil the underlying electronic mechanisms.

Keywords: stress–strain relations, transition-metal elements, γ'-Ni_3Al, first-principles calculations

PACS: 81.40.Jj, 71.20.Be, 31.15.es, 71.15.Mb **DOI:** 10.1088/1674-1056/ab8a38

1. Introduction

As a key strengthening phase of commercial Ni-based single-crystal superalloys, the ordered γ'-Ni_3Al precipitate phase is of great technological importance owing to its excellent elevated-temperature creep and oxidation resistance as well as the anomalous temperature dependence of the yield stress.[1–5] The stoichiometric γ'-Ni_3Al $L1_2$ structure with space group $Pm\bar{3}m$ consists of two sublattices (a face-centered α sublattice occupied by Ni and a cube-corner β sublattice occupied by Al). The mechanical strength of γ'-Ni_3Al can be improved by adding certain ternary alloying elements (*e.g.*, Re, Ta, Ru, W, Ir, and Co).[6–11] Various theoretical studies have focused on the site preference of substitutional ternary elements in γ'-Ni_3Al and the effect of these alloying elements on the elastic properties of the γ' phase at certain Al or Ni sublattice positions. However, the site occupancy behavior of many alloying elements is dependent on the temperature and composition[12–14] owing to the effect of entropy. Consequently, a better understanding of the effect of ternary alloying elements with different sites occupancy on the mechanical properties of γ'-Ni_3Al is fundamental to the practical application of Ni-based single-crystal superalloys.

Various experimental methods can be used to explore the site occupancy of alloying elements in Ni_3Al, including x-ray diffraction, transmission electron microscopy, and atom probe methods.[15–21] However, these experimental studies are costly, and only some transition-metal (TM) elements are considered. Theoretical research on the site preference of alloying elements can make up for the deficiencies of current experimental research methods. Early theoretical investigation was mainly based on the phenomenological Ising-type models.[22–24] For example, Wu *et al.*[23] studied the site preference in ordered $L1_2$-Ni_3Al and observed that the temperature and alloy composition affect the occupancy behavior of alloying elements. Ruban and Skriver[12,25] studied the site occupation of 3d, 4d, and 5d TM elements in the γ' phase using the coherent potential approximation in conjunction with the linear muffin-tin orbitals method. The currently popular theoretical method to calculate the site substitution behavior in ordered compounds is first-principles density functional theory (DFT) calculations using the Wagner–Schottky model.[13,14,18,26–31] By adopting this method, our previous calculations[29] of the site occupancy of TM elements in Ni_3Al indicated that the site behaviors of Fe, Co, Cu, Zn, Ru, Rh, Ag, Cd, and Ir are strongly related to the alloy composition at $T = 0$ K.

*Project supported by the National Natural Science Foundation of China (Grant No. 11804057), the Natural Science Foundation of Guangdong Province, China (Grant No. 2017B030306003), and the National Key Research and Development Program of China (Grant No. 2017YFB0701500).

†Corresponding author. E-mail: hfdong@gdut.edu.cn
‡Corresponding author. E-mail: cywang@mail.tsinghua.edu.cn

© 2020 Chinese Physical Society and IOP Publishing Ltd

Similar to elastic constants, the ideal strength (the minimum stress required to yield a defect-free crystal) of a solid material is a primary intrinsic parameter for understanding the mechanical behaviors of solid structural materials. However, unlike the extensive theoretical efforts devoted to investigating the effect of substitutional TM elements on the elastic properties of the γ'-Ni_3Al phase, the study of the TM-element dependence of the ideal strength of the γ' phase is limited. For $L1_2$-Ni_3Al, the weakest uniaxial tensile direction is the $\langle 110 \rangle$ direction, and the weakest shear slip system is the $\{111\}\langle 11\bar{2} \rangle$ slip system.[32–35] The effects of Re,[32,33] W,[33] Ta,[33] Mo,[33] and Co[33] on the ideal uniaxial tensile strength of γ'-Ni_3Al have been studied using first-principles calculations with the alloying elements occupying the Al sublattice. In Ref. [32], the authors also studied the ideal shear strength of Ni_3Al with and without Re. By combining first-principles calculations and the quasi-harmonic approximation, the temperature-dependent ideal shear strength of the γ' phase doped with alloying elements (Re, Ru, Mo, Cr, Co, W, and Ta) at the Al site was investigated by Wu and Wang.[34] Chen *et al.* studied the site preference and ideal shear strength of γ'-Ni_3Al doped with single Re,[36] single W,[35] double Re,[36] and Re–W[35] using DFT calculations. In our previous study, we investigated the ideal shear strength of Ni_3Al–X (X = 3d:Sc–Zn, 4d:Y–Cd, 5d:Hf–Au) with TM elements occupying the Al site and Ni_3Al–X (X = Ni, Pd, Pt, and Au) with X replacing the Ni atom for $\{111\}\langle 11\bar{2} \rangle$ shear deformation. However, limited attention has been paid to the effect of Ru, Ir, and Fe on the ideal uniaxial tensile behavior of Ni-based superalloys even though these alloying elements play a crucial role in strengthening the mechanical properties of commercial Ni-based superalloys.[9,37–39] Moreover, to the best of our knowledge, there have been no theoretical studies on the dependence of the tensile behavior on the site occupancy of ternary additions (*e.g.*, Co, Ru, Ir, Rh, and Fe) in γ'-Ni_3Al.

In light of this background, the key purpose of the present research is to investigate the effect of Fe, Co, Cu, Zn, Ru, Rh, Ag, Cd, and Ir additions on the ideal shear and uniaxial tensile strengths with different site occupancies in γ'-Ni_3Al using *ab initio* calculations. In addition, the charge redistribution and the chemical bonding between the alloying elements and host atoms in the tensile and shear processes were analyzed to unveil the underlying electronic mechanism.

2. Computational methods

In this work, we studied tension in the [110] direction (the weakest uniaxial tensile orientation) and shear in the $\{111\}\langle 11\bar{2} \rangle$ slip direction (the weakest shear slip system) for all substitutional γ'-Ni_3Al. Figure 1 shows the original model of a 32-atom $2 \times 2 \times 2$ supercell used in the present study, where the (111) plane is denoted by the yellow shadowed area. To explore the dependence of mechanical properties on the site occupancy of TM elements in γ'-Ni_3Al, we adopted a single-impurity model based on the hypothesis of a dilute alloy.[40] Herein, three types of non-equivalent sites in γ'-Ni_3Al, including an Al site and two Ni sites marked by Ni1 and Ni2 in γ'-Ni_3Al in Fig. 1, were substituted by alloying elements to investigate the effect on the shear and tensile behaviors.

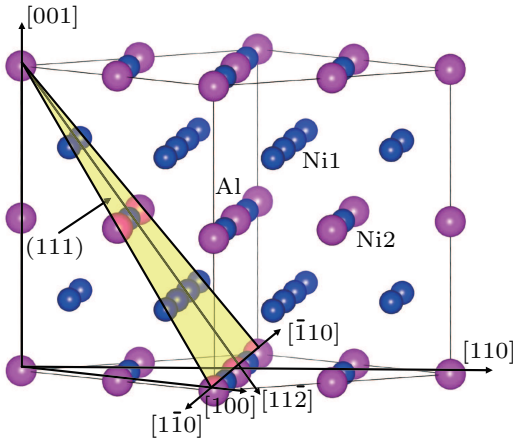


Fig. 1. Schematic illustration of Ni_3Al 32-atom $2 \times 2 \times 2$ supercell. The Al and Ni atoms are denoted by purple and blue balls, respectively. The yellow shadow area represents the (111) slip plane.

By adopting Wagner–Schottky model,[41] our previous study[29] calculated the transfer energy $E_X^{\mathrm{Ni}\to\mathrm{Al}}$ (the energy of moving an X atom from a Ni sublattice to an Al sublattice) of 3d (Sc–Zn), 4d (Y–Cd), and 5d (Hf–Au) TM elements in γ'-Ni_3Al. The results show that the transfer energy of Fe, Co, Cu, Zn, Ru, Rh, Ag, Cd, and Ir is 0.22 eV, 0.74 eV, 0.90 eV, 0.42 eV, 0.04 eV, 0.93 eV, 0.86 eV, 0.28 eV, and 0.54 eV, respectively (shown in Table 3 of Ref. [29]). Since $0 < E_X^{\mathrm{Ni}\to\mathrm{Al}} < E^{\mathrm{ant}}$ (the energy of the exchange antisite defect E^{ant} in γ'-Ni_3Al is determined to be 1.05 eV in our previous study,[29]) the site behaviors of Fe, Co, Cu, Zn, Ru, Rh, Ag, Cd, and Ir are depending on the alloy composition. Hence, we focused on the dependence of mechanical properties on the site occupancy of Fe, Co, Cu, Zn, Ru, Rh, Ag, Cd, and Ir in Ni_3Al in the present research.

To simulate the shear and tensile processes, we adopted the standard approach described in Refs. [26,27]. For [110] uniaxial tension, we set the loading direction along the x axis. Hence, the deformed lattice vector $\boldsymbol{R}$ is given by $\boldsymbol{R} = \boldsymbol{R}_0\boldsymbol{D}$, where $\boldsymbol{R}_0$ is the primitive non-deformed vector, and the tensile deformation matrix $\boldsymbol{D}_{\mathrm{tension}}$ is

$$\boldsymbol{D}_{\mathrm{tension}} = \begin{bmatrix} 1+\varepsilon & 0 & 0 \\ 0 & 1 & 0 \\ 0 & 0 & 1 \end{bmatrix}, \tag{1}$$

where ε is the tensile strain. In terms of $(111)[11\bar{2}]$ shear deformation, the slip plane (111) is rotated normal to the z axis, and the shear direction $[11\bar{2}]$ is rotated parallel to the x axis.

Herein, the $(111)[11\bar{2}]$ shear deformation matrix $\boldsymbol{D}_{\text{shear}}$ is

$$\boldsymbol{D} = \begin{bmatrix} 1 & 0 & 0 \\ 0 & 1 & 0 \\ \gamma & 0 & 1 \end{bmatrix}, \tag{2}$$

where γ is the shear strain. The tensile stress σ and shear stress τ are given by[42,43]

$$\sigma = \frac{1}{V(\varepsilon)} \frac{\partial E}{\partial \varepsilon}, \tag{3}$$

$$\tau = \frac{1}{V(\gamma)} \frac{\partial E}{\partial \gamma}, \tag{4}$$

respectively, where E is the total energy, and $V(\varepsilon)$ and $V(\gamma)$ are the volume of the calculated system at a given tensile strain ε and shear strain γ, respectively.

In the present study, the lattice vector was deformed from 0.0 to 0.18 and 0.28 in steps of 0.02 for the tensile and shear process, respectively. The structures of all the calculated systems were completely relaxed until reaching the force and energy criteria at each deformed strain. The stress–strain relationship was obtained from the calculated tensile and shear energies using Eqs. (3) and (4). As verified in our previous studies,[33,44] the mechanical stability of the crystal lattice of γ'-Ni_3Al will be maintained until the first maximum point of the stress–strain curve during [110] tensile and $(111)[11\bar{2}]$ shear deformation. If there is no other instability mode (*e.g.*, soft phonon instability or magnetic spin arrangement[45–48]), the corresponding stress of this peak point, denoted by σ_{FM} and τ_{FM} respectively, for the tensile and shear process, is exactly the ideal strength of γ'-Ni_3Al under the specified loading. Herein, the corresponding strain of the peak point of the stress–strain curve is defined as the first maximum strain (expressed by ε_{FM} and γ_{FM} for tensile and shear deformation, respectively). In general, first-principles phonon calculations based on DFT are time consuming and were not performed in this work. Thus, our determined ideal strength may be overestimated as the other stability modes were not verified in the present work.

The DFT calculations were performed using the Vienna *Ab Initio* simulation package (VASP)[49] with projector augmented-wave (PAW) pseudopotentials[50] for all calculations. The exchange–correlation functional was described by the Perdew–Burke–Ernzerhof (PBE) generalized gradient approximation (GGA).[51] A Monkhorst–Pack[52] k-mesh of $11 \times 11 \times 11$ was adopted in this work, and the plane-wave kinetic energy cutoff was set to 400 eV. The crystal structure was relaxed until the force converged to less than 0.01 eV/Å, and the energy convergence for electronic self-consistency was 10^{-5} eV.

3. Results and discussion

Dominated by the behavior of chemical bonding, common slip, and nucleation of dislocations,[53–55] the ideal strength of solid materials sets the upper bound of the strength achievable by a real material under certain loading conditions. Investigations of the ideal strength are fundamental to understand the behavior of fracture, failure,[56–58] and creep[59,60] for advanced materials as well as to determine the gap between the real strength of materials and their ideal strength.[61] *Ab initio* computational [110] tensile and $\{111\}\langle 11\bar{2}\rangle$ shear tests were implemented in stoichiometric Ni_3Al, and the ideal strength and corresponding strains calculated according to Eqs. (3) and (4) are presented in Table 1. The maximum stress for the non-doped Ni_3Al ($\sigma_{\text{FM}} = 7.20$ GPa) was achieved at a strain of 8% for [110] tension, and the peak stress ($\tau_{\text{FM}} = 5.84$ GPa) was achieved at a strain of 18% for $\{111\}\langle 11\bar{2}\rangle$ shear. As observed in Table 1, we almost exactly reproduced the ideal strengths for γ'-Ni_3Al for both tensile and shear processes determined in earlier studies,[32,34] except for the work of Chen *et al.*[36]

Table 1. Calculated ideal strengths (in unit GPa) and corresponding strains of Ni_3Al alloys doped with alloying element, along with other DFT predicted values.

System	$\sigma_{\text{FM}}/\varepsilon_{\text{FM}}$ of [110] tension			$\tau_{\text{FM}}/\gamma_{\text{FM}}$ of $(111)[11\bar{2}]$ shear		
Non-doped	7.20/0.08 7.40/0.08[a]			5.84/0.18	5.80/0.18[a] 4.23/0.18[c]	5.768/0.18[b] 5.848/0.18[d]
	Substitutional sublattice			Substitutional sublattice		
	Al	Ni1	Ni2	Al	Ni1	Ni2
Fe	8.33/0.10	6.99/0.08	7.47/0.08	6.27/0.18	5.73/0.16	5.85/0.18
Co	7.38/0.08	7.11/0.08	7.55/0.08	5.81/0.18	5.75/0.16	5.89/0.18
Cu	6.40/0.08	7.78/0.10	7.16/0.08	5.37/0.18	6.11/0.18	5.66/0.18
Zn	6.76/0.08	8.49/0.10	6.91/0.08	5.55/0.18	6.49/0.18	5.47/0.18
Ru	8.80/0.10	6.35/0.08	7.63/0.08	6.54/0.18	5.44/0.16	5.89/0.18
Rh	7.36/0.08	6.72/0.08	7.64/0.08	5.76/0.18	5.51/0.16	5.89/0.18
Ag	6.12/0.08	7.41/0.10	6.86/0.08	5.13/0.16	5.89/0.18	5.46/0.18
Cd	6.48/0.08	8.01/0.10	6.63/0.08	5.39/0.18	6.22/0.18	5.30/0.18
Ir	8.27/0.10	7.01/0.08	7.80/0.08	6.28/0.18	5.71/0.16	6.02/0.18

[a]Ref. [32], [b]Ref. [34], [c]Ref. [36], [d]Ref. [44].

The tensile and shear behavior of X_s-doped Ni_3Al, where X_s denotes the TM elements X (X = Fe, Co, Cu, Zn, Ru, Rh, Ag, Cd, and Ir) occupying the s site (s = Al, Ni1, and Ni2 sites), were systematically studied in this work. The calculated ideal strengths for all the substitutional systems are summarized in Table 1. It can be seen that the ideal strengths of γ' phase doped with different TM elements and a certain X-doped Ni_3Al with the alloying element occupying different sublattices all show significant diversity.

When TM elements X occupied the Al site, according to Table 1, Fe, Ru, and Ir clearly improve σ_{FM} of the γ' phase, with Ru resulting in the greatest enhancement, followed by Fe and Ir. The doping of Co and Rh will slightly increase the ideal tensile strength, whereas the addition of Cu, Zn, Ag, and Cd will weaken σ_{FM} of γ'-Ni_3Al. In terms of $\{111\}\langle 11\bar{2}\rangle$ shear, the TM elements have a similar effect on the ideal shear strength when they occupy the Al site. The effect of the alloying elements on τ_{FM} is in the order: Ru > Ir > Fe > Co > Rh > Zn > Cd > Cu > Ag. Ru, Ir, and Fe clearly improve the ideal shear strength of γ'-Ni_3Al, whereas alloying elements with fully filled d shells such as Cu ($3d^{10}4s$), Zn ($3d^{10}4s^2$), Ag ($4d^{10}5s$), and Cd ($4d^{10}5s^2$) are expected to decrease τ_{FM}, with Ag exhibiting the strongest decreasing effect. Unlike the effect of Rh and Co on the ideal tensile strength, Rh and Co will slightly decrease the ideal shear strength of the γ' phase.

Compared with Al-site defected alloys, Ni-site defected Ni_3Al results in a different scenario. There are two non-equivalent Ni sites in γ'-Ni_3Al: the Ni1 site of the $[\bar{1}10]$ crystal column composed of only Ni atoms and the Ni2 site of the $[\bar{1}10]$ crystal column composed of Ni and Al atoms (see Fig. 1). Hence, we evaluated the *ab initio* [110] tensile and $\{111\}\langle 11\bar{2}\rangle$ shear deformations for both X_{Ni1}-doped and X_{Ni2}-doped alloys in the present study. As demonstrated in Table 1, if a certain alloying element X improves τ_{FM} and σ_{FM} when occupying the Ni1 site, this element will decrease τ_{FM} and σ_{FM} when occupying the Ni2 site, and *vice versa.* None of the studied elements could simultaneously increased the ideal strength of the γ' phase for both Ni1-site and Ni2-site substitution. Elements with partially filled d orbitals, *i.e.*, Fe ($3d^64s^2$), Co ($3d^74s^2$), Ru ($4d^75s$), Rh ($4d^85s$), and Ir ($5d^76s^2$), resulted in a decrease of τ_{FM} and σ_{FM} when occupying the Ni1 site, whereas they enhanced the ideal tensile and shear strength of γ' alloys when occupying Al site and Ni2 site. In contrast, the elements with fully filled d-shells (*i.e.*, Cu, Zn, Ag, and Cd) possessed the opposite strengthening efficacy on the ideal strength of γ'-Ni_3Al.

To better illustrate the effect of the ternary alloying additions on the ideal strength of Ni_3Al alloys, the relations between $\Delta\sigma_{FM}$ and $\Delta\tau_{FM}$ (both expressed in percent of the ideal strength of stoichiometric Ni_3Al) are plotted in Fig. 2, where $\Delta\sigma_{FM}$ and $\Delta\tau_{FM}$ represent the difference in σ_{FM} and τ_{FM}, respectively, between Ni_3Al–X alloys and non-doped Ni_3Al (*i.e.*, $\Delta\sigma_{FM} = \sigma_{FM}^{Ni_3Al-X} - \sigma_{FM}^{Ni_3Al}$ and $\Delta\tau_{FM} = \tau_{FM}^{Ni_3Al-X} - \tau_{FM}^{Ni_3Al}$). Although the effects of different TM elements on the ideal strength of γ'-Ni_3Al varied, as described in Fig. 2, a linear relationship for $\Delta\sigma_{FM}$ *versus* $\Delta\tau_{FM}$ can be observed when the TM elements occupy the same s site (*i.e.*, Al-, Ni1-, or Ni2-site). The slope of the linear fit is 1.60, 1.58, and 1.33 for Al-site, Ni1-site, and Ni2-site defected alloys, respectively. Thus, it can be expected that the effect of alloying elements on the ideal tensile strength is overall greater than the effect on the ideal shear strength. Among all the calculated substitutional systems, Ni_3Al with Ru occupying the Al site exhibited the greatest σ_{FM} and τ_{FM}, whereas Ni_3Al with Ag occupying the Al site displayed the smallest σ_{FM} and τ_{FM} (see Fig. 2 and Table 1).

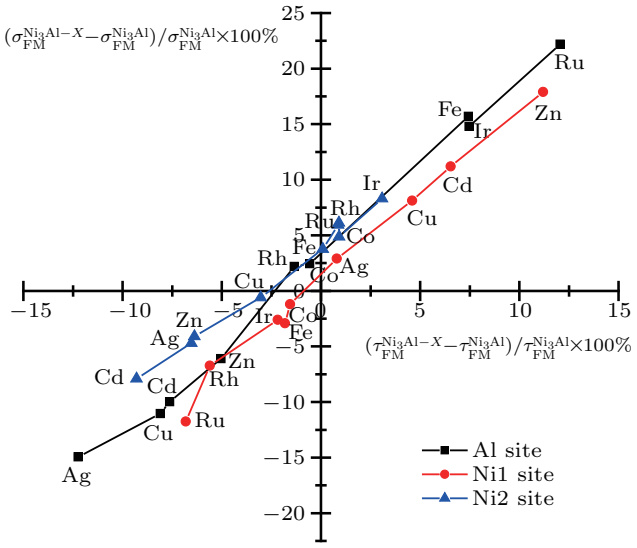


Fig. 2. Correlations between $(\sigma_{FM}^{Ni_3Al-X} - \sigma_{FM}^{Ni_3Al})/\sigma_{FM}^{Ni_3Al}$ expressed in percent (%) and $(\tau_{FM}^{Ni_3Al-X} - \tau_{FM}^{Ni_3Al})/\tau_{FM}^{Ni_3Al}$ expressed in percent (%) for all calculated Ni_3Al alloys. The black squares, red circles, and blue triangles represent systems with TM elements substituting the Al site, Ni1 site, and Ni2 site, respectively.

To obtain deeper insight into the underlying electronic mechanism responsible for the various efficiencies of ternary alloy element additions on the tensile and shear behavior, we investigated the charge redistribution induced by the substitutional impurities in γ'-Ni_3Al during the tensile and shear processes. Figures 3(a)–3(i) presents the charge density differences ($\Delta\rho$) of the $(\bar{1}10)$ plane containing a ternary alloying element for Ru_{Al}-doped and Zn_{Al}-doped Ni_3Al alloys (*i.e.*, $Ni_{24}Al_7Ru$ and $Ni_{24}Al_7Zn$) along with non-doped Ni_3Al at different loading strains.

As observed in Figs. 3(a)–3(c), compared with $\Delta\rho$ of non-doped Ni_3Al, the electrons of $Ni_{24}Al_7Ru$ are clearly accumulated around the Ru atom flowing from both Ru and its first nearest neighbor (FNN) host atoms (*i.e.*, Ni atoms), and

$\Delta\rho$ exhibits robust directionality (mainly appearing along the [110] direction) at zero strain. In contrast, $\Delta\rho$ of the Zn_{Al}-doped system shows completely different behavior: Zn doping does not enhance the electron accumulation, and the bonding between Zn and the host atoms shows obvious metallic character. Consequently, the substitution of Ru on the Al site enhances the mechanical properties of Ni_3Al alloys, whereas the doping of Zn on the Al site weakens the mechanical behavior, which is consistent with our previous calculations of σ_{FM} and τ_{FM} (see Table 1 and Fig. 2) and previous experimental results.[9,37–39] Herein, it can be predicted that the bonding character of Fe–Ni and Ir–Ni bonds will be similar to that of the Ru–Ni bond, whereas the interactions of the fully filled d-shell elements (*i.e.*, Cu, Ag, and Cd) and Ni atoms will be similar to those of Zn–Ni bonds. Indeed, Ru, Ir, and Fe are important elements in practical commercial Ni-based superalloys.[1–3,9,37–39] As the strains increase under [110] tension, the distances between atoms along the loading orientation increase, whereas the bond length between atoms along the [001] direction (the perpendicular direction to the applied strain) decreases. Hence, the charge density difference of $Ni_{24}Al_7Ru$, $Ni_{24}Al_7Zn$, and stoichiometric Ni_3Al along the [110] direction are significantly weakened at a tensile strain of 8% (see Figs. 3(d)–3(f)).

Figures 3(g)–3(i) display $\Delta\rho$ of the $(\bar{1}10)$ plane at a strain of $\gamma = 18\%$ during $\{111\}\langle 11\bar{2}\rangle$ shear deformation for $Ni_{24}Al_7Ru$, $Ni_{24}Al_7Zn$, and non-doped Ni_3Al. With increasing shear strain, the bonding in the $[11\bar{2}]$ direction becomes weaker for all the calculated systems. As observed in Figs. 3(d)–3(i), $\Delta\rho$ in the Ru_{Al}-doped system exhibited stronger charge accumulation than non-doped Ni_3Al, and $\Delta\rho$ of the Zn_{Al}-doped system was the weakest. Moreover, the Ru_{Al}-doped system has the strongest covalent-like bonds (*i.e.*, Ru–Ni bonds), followed by non-doped Ni_3Al, with the weakest bonds observed for the Zn_{Al}-doped system. Doping of Ru on the Al site in γ'-Ni_3Al can significantly strengthen the shear strength of the alloys, whereas substitution of Zn on the Al site weakens the shear strength of the system.

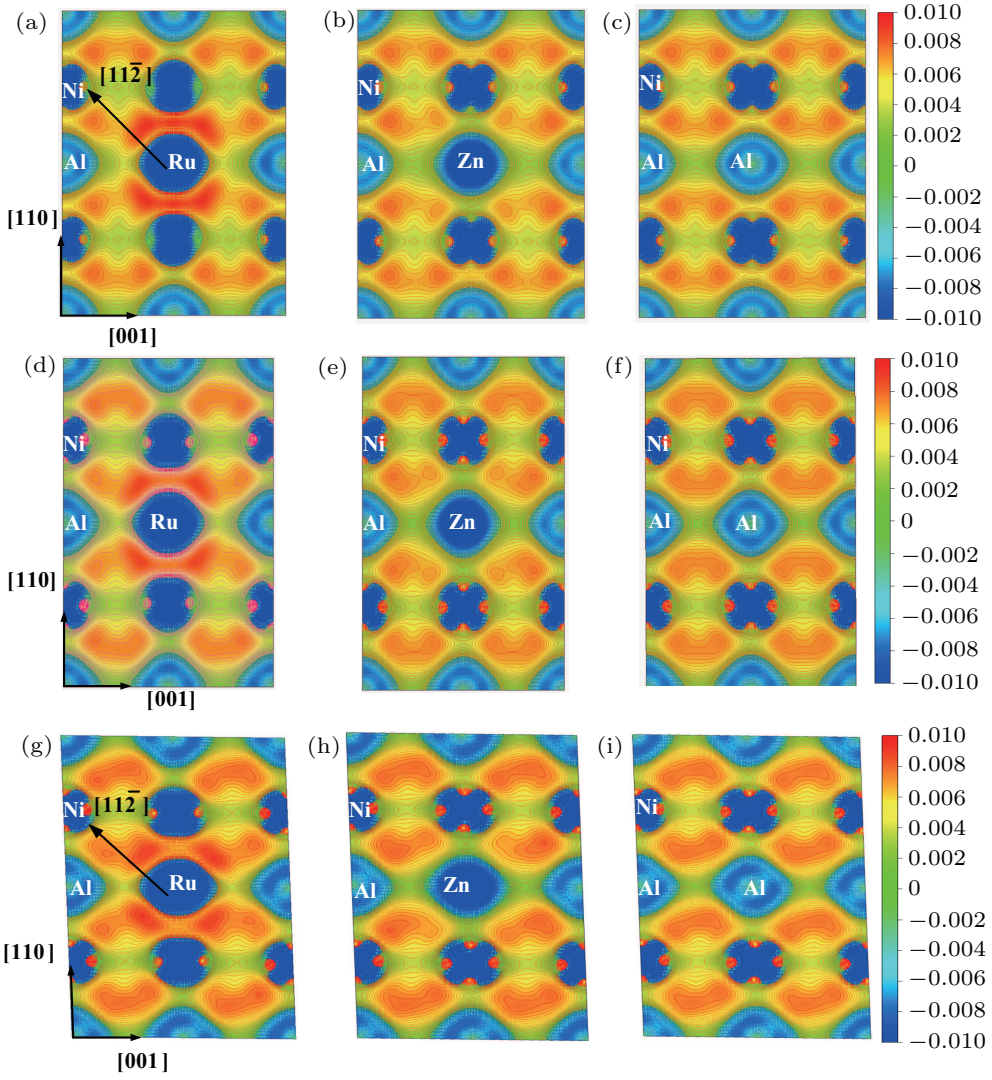


Fig. 3. Charge density difference of $(\bar{1}10)$ plane containing the alloying element for $Ni_{24}Al_7Ru$, $Ni_{24}Al_7Zn$, and stoichiometric Ni_3Al at [(a)–(c)] a strain of 0%, [(d)–(f)] a tensile strain of 8%, and [(g)–(i)] a shear strain of 18%. Positive (negative) values [e/(a.u.)^3] denote charge accumulation (depletion).

In terms of Ni-site defect alloys, the ideal tensile and shear strength are dependent on the ternary elements as well as the doping site. To reveal the strengthening mechanism, we also studied the variation of the bond lengths between the TM element X (X = Ru, Zn, and Ni) and its FNN host atoms in $Ni_{23}Al_8Ru$, $Ni_{23}Al_8Zn$, and stoichiometric Ni_3Al during the uniaxial tensile processes. At zero strain, the impurity atom X possesses 12 FNN atoms consisting of 4 Al atoms, 4 Ni1 atoms, and 4 Ni2 atoms (see insets of Fig. 4). With increasing loading strain, the bond length along the [110] tensile direction increases, whereas the bond length along the [101] orientation decreases for all the studied alloys. Consequently, the shortest X–Ni bonds are along the [101] direction during the tensile process for both X_{Ni1}-doped and X_{Ni2}-doped alloys. The bond lengths of X_s–Ni bonds (X = Ru and Zn, s = Ni1 and Ni2 site), denoted by $L(X-Ni)$, along the [101] direction in X_s-doped Ni_3Al as a function of tensile strain are plotted in Fig. 4. The bond lengths of the Ni–Ni bond along the [101] direction of pure Ni_3Al are also plotted in Fig. 4 for comparison.

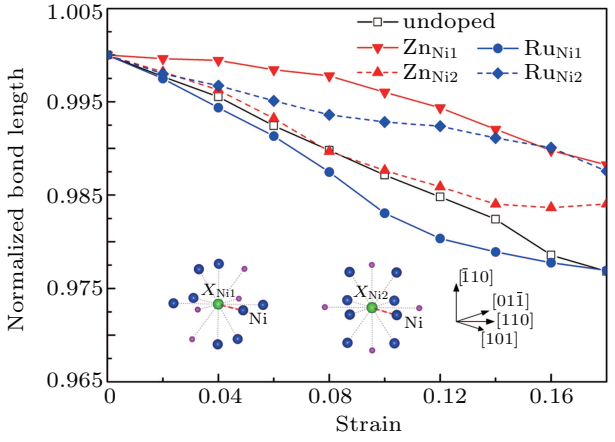


Fig. 4. Variation of bond lengths between the TM element X (X = Ru, Zn, and Ni) and its FNN host atoms normalized with respect to their respective equilibrium values during [110] tensile tests for $Ni_{23}Al_8Ru$, $Ni_{23}Al_8Zn$, and stoichiometric Ni_3Al. The left (right) inset shows the substitutional impurity atom X and its FNN atoms for X_{Ni1}-doped (X_{Ni2}-doped) alloys at zero strain. The purple, blue, and green balls represent Al, Ni, and X atoms, respectively. The red dashed lines in the insets mark the shortest X–Ni bond during the tensile loading.

As demonstrated in Fig. 4, with the application of tensile strain step by step in pure Ni_3Al, the bond length of the Ni–Ni bond, L(Ni–Ni), in the [101] direction decreases and contracts to 0.9898 times the original length at the peak strain of 8%. For Ru-doped Ni_3Al, the shrinkage of L(Ru–Ni) at the strain of 8% varies with the Ni site occupancy. Compared with non-doped Ni_3Al, the length of the Ru–Ni bond in X_{Ni1}-doped Ni_3Al decreases much more, whereas L(Ru–Ni) in X_{Ni2}-doped Ni_3Al decreases much less. It can be predicted that Ru doping can effectively improve (weaken) the deformation resistance and mechanical properties of Ni_3Al alloys when Ru occupies the Ni2 (Ni1) site, which is consistent with our previous calculations of ideal tensile strength (see Table 1 and Fig. 2). For Zn-doped systems, the opposite is true. The length of the Zn–Ni bond in the [101] orientation contracts to 0.9978 times and 0.9896 times the original at a strain of 8% for the Ni1-site and Ni2-site defect model, respectively. Consequently, Zn_{Ni1}-doped alloys exhibit a much higher σ_{FM} than pure Ni_3Al and Zn_{Ni2}-doped alloys exhibit a slightly smaller σ_{FM} than non-doped Ni_3Al, which agrees well with our calculated results in Table 1 and Fig. 2.

4. Conclusions

The effects of Fe, Co, Cu, Zn, Ru, Rh, Ag, Cd, and Ir on the ideal shear and uniaxial tensile behaviors with different site occupancy in γ'-Ni_3Al were studied in detail using *ab initio* total-energy methods. Our results indicate that the dependence of the ideal strength on the site preference of alloying element X in γ'-Ni_3Al is associated with the d-shell occupancy of X. Elements with partially filled d orbitals (*i.e.*, Fe, Co, Ru, Rh, and Ir) enhance the ideal tensile strength when occupying the Al site in Ni_3Al, whereas elements with fully filled d orbitals (*i.e.*, Cu, Zn, Ag, and Cd) lead to a decrease of τ_{FM} and σ_{FM}. Furthermore, the strengthening effect of Ru arises from the covalent-like bonds between impurities and host atoms according to analysis of the charge redistribution of Ni_3Al alloys, whereas the detrimental effect of Zn is caused by the metallic bonds between Zn and Ni. In terms of Ni-site defect Ni_3Al, elements with partially filled d shells are expected to weaken (improve) the ideal tensile and shear strength of the alloys when they occupy the Ni1 (Ni2) site, and the elements with fully filled d shells have the reverse effect. Moreover, the variations of the bond lengths between the TM element X (X = Ru, Zn, and Ni) and its FNN host atoms during uniaxial tensile tests indicate that Ru can effectively enhance (weaken) the deformation resistance and mechanical behaviors of the γ' phase when occupying the Ni2 (Ni1) site, whereas the opposite is true for Zn. In addition, a linear relationship for $\Delta\sigma_{FM}$ *versus* $\Delta\tau_{FM}$ was observed for the alloys with Al-, Ni1-, and Ni2-site defects in this study. Our findings provide insight into the reinforcement effects of ternary alloying elements on the ideal strength with different site preferences in γ'-Ni_3Al, which have not been previously studied using first-principles calculations.

Acknowledgments

The simulations were performed on the "Lvliang" cluster system of the National University of Defense Technology, Hunan, China. The authors would like to thank Tiffany Jain M S, from Liwen Bianji, Edanz Group China (www.liwenbianji.cn/ac), for editing the English text of this manuscript.

References

[1] Sims C T, Stoloff N S and Hagel W C 1987 *Superalloys II* (New York: John Wiley & Sons)
[2] Reed R C 2006 *The superalloys: fundamentals and applications* (New York: Cambridge university Press)
[3] Loria E A 1989 *Superalloy 718: metallurgy and applications* (Warrendale, PA: TMS) p. 1989
[4] Karnthaler H, Mühlbacher E T and Rentenberger C 1996 *Acta Materialia* **44** 547
[5] Pollock T M and Tin S 2006 *J. Propulsion Power* **22** 361
[6] Reed R, Tao T and Warnken N 2009 *Acta Mater.* **57** 5898
[7] Nathal M and Ebert L 1985 *Metall. Trans. A* **16** 1863
[8] Fleischmann E, Miller M K, Affeldt E and Glatzel U 2015 *Acta Mater.* **87** 350
[9] Yeh A C and Tin S 2005 *Scr. Materialia* **52** 519
[10] Fahrmann M, Hermann W, Fahrmann E, Boegli A, Pollock T and Sockel H 1999 *Mater. Sci. Eng. A* **260** 212
[11] Liu Z and Gao W 2001 *Oxidation Metals* **55** 481
[12] Ruban A V and Skriver H L 1997 *Phys. Rev. B* **55** 856
[13] Jiang C and Gleeson B 2006 *Scr. Materialia* **55** 433
[14] Jiang C, Sordelet D and Gleeson B 2006 *Acta Mater.* **54** 1147
[15] Rüsing J, Wanderka N, Czubayko U, Naundorf V, Mukherji D and Rösler J 2002 *Scr. Mater.* **46** 235
[16] Mottura A, Warnken N, Miller M K, Finnis M W and Reed R C 2010 *Acta Mater.* **58** 931
[17] Reed R C, Yeh A C, Tin S, Babu S S and Miller M K 2004 *Scr. Materialia* **51** 327
[18] Zhou Y, Mao Z, Booth-Morrison C and Seidman D N 2008 *Appl. Phys. Lett.* **93** 171905
[19] Amouyal Y, Mao Z, Booth-Morrison C and Seidman D N 2009 *Appl. Phys. Lett.* **94** 041917
[20] Bagot P A J, Silk O B W, Douglas J O, Pedrazzini S, Crudden D J, Martin T L, Hardy M C, Moody M P and Reed R C 2017 *Acta Mater.* **125** 156
[21] Lin H and Pope D P 1990 *J. Mater. Res.* **5** 763
[22] Ochial S, Oya Y and Suzuki T 1984 *Acta Metall.* **32** 289
[23] Wu Y P, Tso N C, Sanchez J M and Tien J K 1989 *Acta Metall.* **37** 2835
[24] Sluiter M H F and Kawazoe Y 1995 *Phys. Rev. B* **51** 4062
[25] Ruban A V and Skriver H L 1996 *Solid State Commun.* **99** 813
[26] Kim D E, Shang S L and Liu Z K 2010 *Intermetallics* **18** 1163
[27] Wu Q and Li S 2012 *Comput. Mater. Sci.* **53** 436
[28] Ruban A V, Popov V A, Portnoi V K and Bogdanov V I 2014 *Philos. Mag.* **94** 20
[29] Wen M and Wang C Y 2018 *Phys. Rev. B* **97** 024101
[30] Liu S, Li Z and Wang C 2017 *Chin. Phys. B* **26** 093102
[31] Lu B, Wang C Y and Du Z 2018 *Chin. Phys. B* **27** 097102
[32] Wang Y J and Wang C Y 2009 *Scr. Mater.* **61** 197
[33] Wen M and Wang C Y 2016 *RSC Adv.* **6** 77489
[34] Wu X and Wang C 2016 *RSC Adv.* **6** 20551
[35] Chen Y, He S, Yi Z and Peng P 2019 *J. Phys. Chem. Solids* **131** 34
[36] Chen Y, He S, Yi Z and Peng P 2018 *Comput. Mater. Sci.* **152** 408
[37] Heckl A, Neumeier S, Göken M and Singer R 2011 *Mater. Sci. Eng. A* **528** 3435
[38] Tan X, Liu J, Jin T, Hu Z, Hong H, Choi B, Kim I, Jo C and Mangelinck D 2013 *Mater. Sci. Eng. A* **580** 21
[39] Han Y F, Ma W Y, Dong Z Q, Li S S and Gong S K 2008 *Superalloys. Pennsylvania PA: TMS* **91**
[40] Wang C Y, Liu S Y and Han L G 1990 *Phys. Rev. B* **41** 1359
[41] Wagner C and Schottky W 1930 *Z. Phys. Chem. B* **11** 163
[42] Roundy D, Krenn C R, Cohen M L and Morris J W Jr 1999 *Phys. Rev. Lett.* **82** 2713
[43] Roundy D, Krenn C R, Cohen M L and Morris J W Jr 2001 *Philos. Mag. A* **81** 1725
[44] Wen M, Xie X, Gao Y, Dong H, Mu Z, Wu F and Wang C Y 2019 *J. Alloys Compd.* **806** 1260
[45] Clatterbuck D M, Krenn C R, Cohen M L and Morris J W Jr 2003 *Phys. Rev. Lett.* **91** 135501
[46] Dubois S M M, Rignanese G M, Pardoen T and Charlier J C 2006 *Phys. Rev. B* **74** 235203
[47] Řehák P, Černý M and Šob M 2015 *Modell. Simul. Mater. Sci. Eng.* **23** 055010
[48] Wen M and Wang C Y 2017 *Chin. Phys. B* **26** 093106
[49] Kresse G and Furthmüller J 1996 *Phys. Rev. B* **54** 11169
[50] Kresse G and Joubert D 1999 *Phys. Rev. B* **59** 1758
[51] Perdew J P, Burke K and Ernzerhof M 1996 *Phys. Rev. Lett.* **77** 3865
[52] Monkhorst H J and Pack J D 1976 *Phys. Rev. B* **13** 5188
[53] Kelly A and Macmillan N 1986 *Strong Solids* (Oxford: Clarendon)
[54] Clatterbuck D M, Chrzan D C and Morris J W 2003 *Acta Mater.* **51** 2271
[55] Jokl M, Vitek V and McMahon C Jr 1980 *Acta Metall.* **28** 1479
[56] Krenn C R, Roundy D, Morris J W and Cohen M L 2001 *Mater. Sci. Eng. A* **319** 111
[57] Chrzan D C, Sherburne M P, Hanlumyuang Y, Li T and Morris J W Jr 2010 *Phys. Rev. B* **82** 184202
[58] Sawyer C A, Morris J W Jr and Chrzan D C 2013 *Phys. Rev. B* **87** 134106
[59] Joos B and Duesbery M 1997 *Phys. Rev. Lett.* **78** 266
[60] Tian S, Wu J, Shu D, Su Y, Yu H and Qian B 2014 *Mater. Sci. Eng. A* **616** 260
[61] Pokluda J, Černý M, Šob M and Umeno Y 2015 *Prog. Mater. Sci.* **73** 127